K. A. Peleaux, T.-P. K. Nguyen, A. Anton, and C. T.-C. Nguyen, "A parametric MEMS oscillator-based super-regenerative receiver front-end," *Proceedings*, IEEE Int. Frequency Control Symp., Orlando, Florida, April 14-18, 2019, DOI: 10.1109/FCS.2019.8856028.

A Parametric MEMS Oscillator-Based Super-Regenerative Receiver Front-End

Kieran A. Peleaux, Thanh-Phong K. Nguyen, Alain Antón, Zeying Ren, and Clark T.-C. Nguyen

Berkeley Sensor & Actuator Center
Dept. of Electrical Engineering and Computer Sciences
University of California at Berkeley
Berkeley, California, USA

***Abstract*—The use of parametric oscillator start-up principles applied to a MEMS-based super-regenerative receiver front-end obviates the need for a positive feedback sustaining amplifier and permits OOK input detection with sensitivity better than −67 dBm using only 15 µW of pump power, which is 33 times smaller than the previous published mark of 490 µW using MEMS [1]. Here, removal of the sustaining amplifier (and its 489 µW) and instigation of oscillator start-up via parametric means permit use of a much lower power oscillator, e.g., a ring oscillator, to pump the RF front-end detecting resonator at double its resonance frequency while retaining acceptable receiver sensitivity. The substantial reduction in power consumption afforded by this method is compelling for IoT applications, where power is paramount, especially for wireless communications.**

Keywords—MEMS, micromechanical resonator, parametric oscillator, super-regenerative receiver, wireless front-end, OOK, FSK.

I. Introduction

MEMS-based super-regenerative receivers offer some of the lowest power means for wireless communication, with published OOK receive power consumptions down to 490 µW well below the wake-state 60 mW of Bluetooth LE [1] [2]. The lower power of the MEMS-based approach makes it lucrative for IoT applications, for which bit rates are often low and battery lifetime is paramount. The premium placed on power by this application not only fuels recent efforts to commercialize MEMS-based super-regenerative receivers, but also provides incentive for replacing them when an even lower power approach emerges.

This work explores a strategy to reduce power consumption over that of [1] by dispensing with its sustaining amplifier and instead using parametric oscillation start-up in a super-regenerative front-end via the circuit of Fig. 1. This permits use of a much lower power oscillator, e.g., a ring oscillator, to generate the needed frequency-doubled pump, with more than an order of magnitude in potential power savings in today's CMOS [3] [4].

II. Super-Regenerative Receiver Working Principle

The basic concept behind a super-regenerative receiver front-end is to attain large amplification gain by repeatedly routing a signal through the same (low gain A_v) amplifier N times, which effectively achieves a gain of A_v^N [5]. This of course describes what an oscillator does, the only difference being that instead of starting-up from just noise, the super-regenerative circuit starts up from an injected input signal, perhaps via an antenna as shown in Fig. 2, which depicts the front-end implementation of [1]. Here, the amplifier placed in feedback with the frequency-selective element—in this case a MEMS wine-glass disk resonator—is a quenching amplifier that periodically switches on and off to allow for repeated oscillation growth cycles. In the absence of an injected signal, the oscillation growth is slow, since it starts up from just noise. On the other hand, the presence of an injected signal effectively kicks initial energy into the oscillator loop, allowing much faster oscillation start-

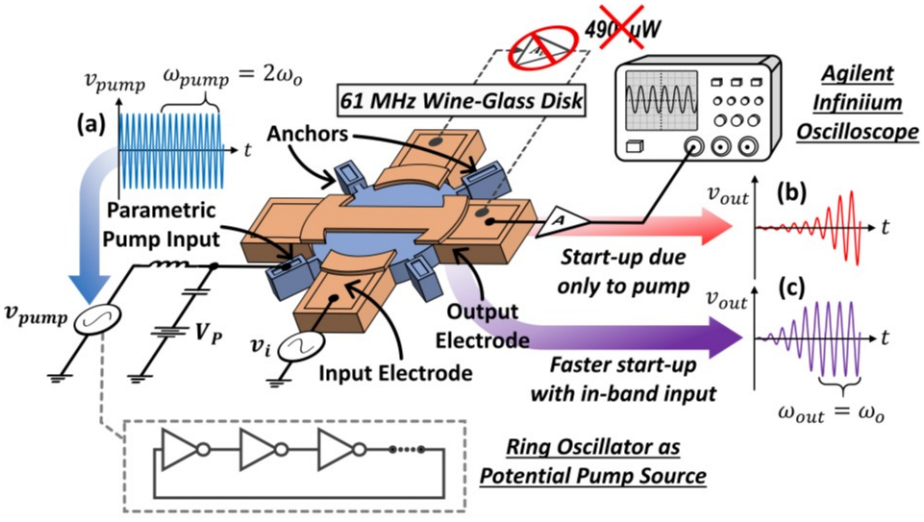

Fig. 1: Perspective view of a wine-glass disk resonator hooked up as a parametric oscillator-based super-regenerative receiver front-end. The waveforms depict (a) the parametric pump (blue) at twice the device's resonance frequency, ω_o, (b) the output oscillation growth due only to the pump (red), and (c) the much faster growth (purple) that occurs in the presence of an input signal at frequency ω_o.

K. A. Peleaux, T.-P. K. Nguyen, A. Anton, and C. T.-C. Nguyen, "A parametric MEMS oscillator-based super-regenerative receiver front-end," *Proceedings*, IEEE Int. Frequency Control Symp., Orlando, Florida, April 14-18, 2019, DOI: 10.1109/FCS.2019.8856028.

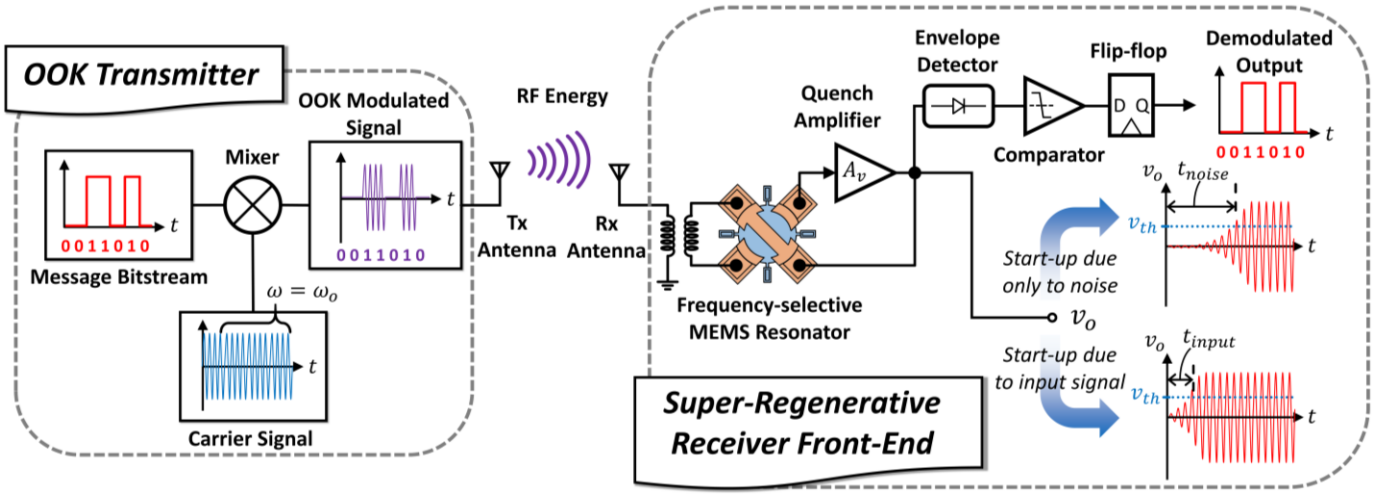

Fig. 2: Schematic of the super-regenerative receiver front-end previously demonstrated in [1]. Here, a binary message is encoded via on-off keying (OOK) modulation of a carrier signal at ω_o and subsequently transmitted to the super-regenerative receiver. In the front-end, the frequency-selective tank in positive feedback with a sustaining amplifier allows noise to grow into oscillations, which are then periodically quenched. The growth of the oscillations is much faster upon injection of an input signal at the disk resonance frequency via the antenna (the '1' regions in the waveforms). Thresholding decision-making circuits then demodulate based on the growth rate of oscillation.

up. The difference in time necessary to reach a certain threshold of oscillation amplitude then provides a framework by which to assign binary bits, e.g., assign a '0' to slow start-up and a '1' to fast start-up.

For the specific OOK reception used in [1] (and here) with input waveform shown in Fig. 2, a transmitted '0' presents no energy, while a transmitted '1' comprises a sinusoid within the resonance passband of the MEMS resonator. The lack of injected energy for the '0' case leads to slow oscillation growth, so the receiver outputs a '0' when the time needed for the envelope of the oscillator output to surpass a given threshold exceeds the quenching period, i.e., when the signal amplitude never reaches the threshold by the time the quenching cycle finishes.

The super-regenerative front-end of [1], shown in Fig. 2, used a 4-port MEMS-based wine-glass disk resonator to not only accept received OOK signal inputs, but also filter them and then inject them into the oscillator loop of a super-regenerative circuit driven by a sustaining amplifier. The filtering is such that only signals within the MEMS resonator passband make it to the oscillator loop. This channel-select filtering greatly increases robustness against interferers when compared with conventional super-regenerative receivers that lack front-end channel selection [6]. With a frequency within the resonance passband of the MEMS resonator, the sinusoid denoting a '1' has no problem traversing from the left input electrodes to the right oscillator electrodes, where it injects into the oscillator positive feedback loop. The ensuing injection-assisted oscillation growth reaches the threshold before the quench period ends, at which point thresholding decision-making circuits trigger reception of a '1' by the receiver.

In the Fig. 2 implementation, the envelope detector, comparator, and latch serve as the main threshold-detecting decision-making circuits. They consume relatively negligible energy compared to the sustaining amplifier, which dominates the power consumption, hence the desire to replace the sustaining amplifier with a more efficient alternative.

III. Parametric Super-Regeneration

The parametric super-regenerative front-end demonstrated herein, shown in Fig. 1, removes the closed feedback loop, and instead realizes positive feedback parametrically by pumping the disk resonator structure via a signal at twice its resonance frequency provided by a separate very low power oscillator [7]. Application of the pump signal to the resonant structure leaves one electrode available to receive the input signal (e.g., from an antenna) and the other to direct the growing oscillating output to a following threshold-detecting decision stage.

The principle of parametric oscillation is a well-known phenomenon first discovered through the mechanical resonance of "singing" wine glasses [8]. It has since extended to the electrical domain and is often leveraged in optical parametric oscillators. Parametric oscillation occurs when a resonant system contains a parameter that varies at a frequency different from its resonance frequency. One of the most intuitive examples of this is spinning figure skaters, who must move their limbs inwards and outwards at twice their spinning frequency to maintain their angular momentum. This behavior ultimately equates to modulating the skater's moment of inertia, which allows for sustained rotation.

In the case of a capacitive-gap-transduced MEMS resonator, parametric oscillation begins upon application of a voltage signal across an electrode-to-resonator gap at twice the resonance frequency of the resonator. This signal, through the nonlinear capacitive transducer, generates a time-varying electrical stiffness, which in turn modulates the entire resonant system's effective stiffness [7]. Substituting this time-varying stiffness into the classical mass-spring-damper differential equation and using the method of Hill's infinite determinant yields an inequality that describes the generic condition for parametric oscillation. This expression can then be refined to find the pump amplitude and dc-bias voltages necessary to drive a resonator into

K. A. Peleaux, T.-P. K. Nguyen, A. Anton, and C. T.-C. Nguyen, "A parametric MEMS oscillator-based super-regenerative receiver front-end," *Proceedings*, IEEE Int. Frequency Control Symp., Orlando, Florida, April 14-18, 2019, DOI: 10.1109/FCS.2019.8856028.

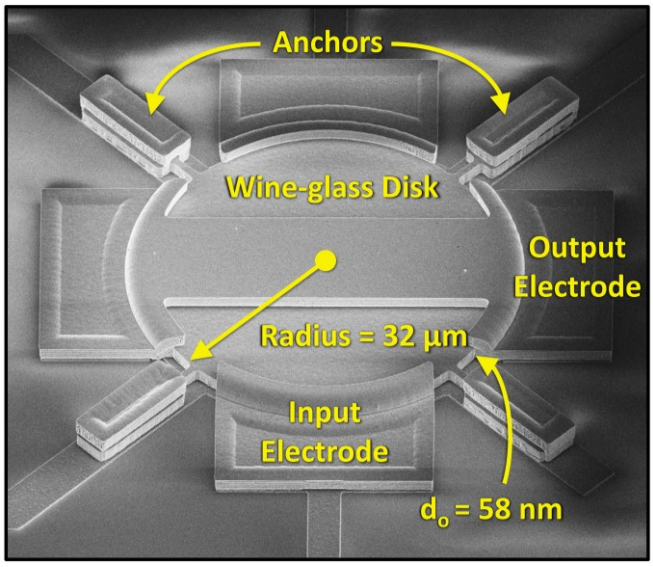

Fig. 3: Scanning electron micrograph of the wine-glass disk resonator used in this work with key dimensions and features labeled.

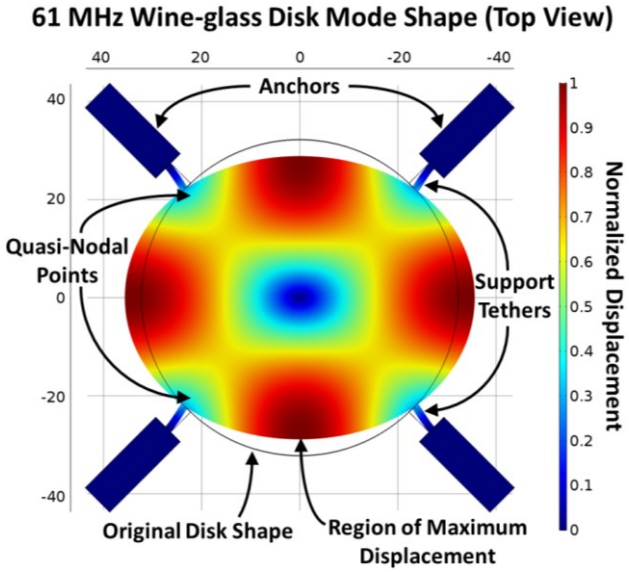

Fig. 4: FEA simulation of a wine-glass disk mode shape with color legend depicting normalized displacement magnitude. Dark blue regions represent no displacement, while dark red regions represent maximum displacement.

parametric oscillation, which takes the form

$$QV_P V_{pump} > 2\frac{\omega_{nom}}{\omega_o} k_{eff} \frac{d_o^2}{\kappa_i^2 C_o} \approx 2k_m \frac{d_o^2}{\kappa_i^2 C_o} \qquad (1)$$

where Q is the resonator quality factor, V_P is the dc-bias voltage, V_{pump} is the voltage amplitude of the pump signal at $2\omega_o$, ω_{nom} is the natural resonance frequency without frequency pulling, ω_o is the resonance frequency with frequency pulling, k_{eff} is the total effective stiffness including both mechanical and electrical components, k_m is the purely mechanical stiffness, d_o is the electrode-to-resonator gap, κ_i is a scaling factor to account for non-uniform displacement along the electrode length [9], and C_o is the static electrode-to-resonator capacitance [10].

Driving the high-Q resonator into oscillation solely via this effect takes longer than the typical method of applying a time-varying voltage at the resonance frequency ω_o. Just as for a traditional super-regenerative receiver though, in the presence of an additional injected input signal at frequency ω_o, the oscillation grows much faster. Here, the slow growth in absence of an injected input permits larger differences in time-to-threshold of the oscillation envelopes, which can help to delineate between a '0' or a '1'.

IV. MEMS Resonator & Fabrication

This work utilizes a high-Q, 61-MHz polysilicon wine-glass disk resonator [11], depicted in Fig. 3, as both the source of parametric oscillation and as the highly selective front-end filter applied to incoming signals. The resonator consists of a 2-µm-thick, 32-µm-radius disk supported by substrate-anchored tethers attached at four quasi-nodal locations around its circumference. From the (exaggerated) mode shape depicted in Fig. 4**Error! Reference source not found.**, these nodal points undergo minimal displacement when the disk vibrates in its wine-glass mode. This helps to maximize the Q of the device.

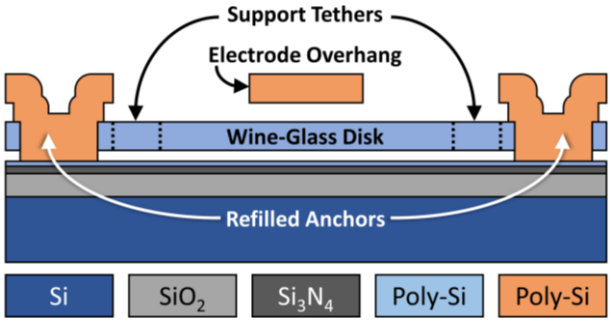

Fig. 5: Final fabrication cross-section of the polysilicon wine-glass disk after anchor refilling with polysilicon and release in HF.

This resonator was fabricated using a process sequence similar to the four-mask, self-aligned stem process of [12], which was originally developed to better align center-supported disk resonator stems to the resonators themselves, reducing anchor losses due to asymmetry. The device in this work is of course not center-supported, but as shown in the process cross-section of Fig. 5, its anchors benefit from the strengthening effect of stem refilling, which also maximizes Q.

During conventional (i.e., non-parametric) operation, shown in Fig. 6 in an actual measurement circuit, the resonator structure is biased with dc voltage V_P and surrounded by four electrodes, two of which are connected physically, and all of which are separated from the resonator disk by a 58 nm gap. The resulting electrode-to-resonator gap capacitors then serve as the input and output capacitive-gap transducers. Application of a time-varying voltage across one of the electrode gaps generates a time-varying force on the resonator structure. If this force is at the resonance frequency ω_o, the resonator will vibrate with significant amplitude, which in turn generates an output current

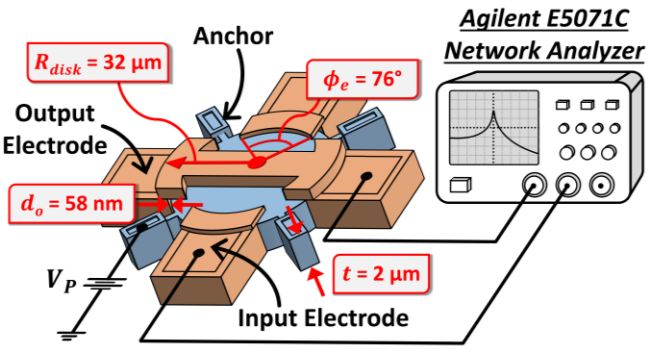

Fig. 6: Perspective view of the wine-glass disk resonator and test setup used to measure its frequency response.

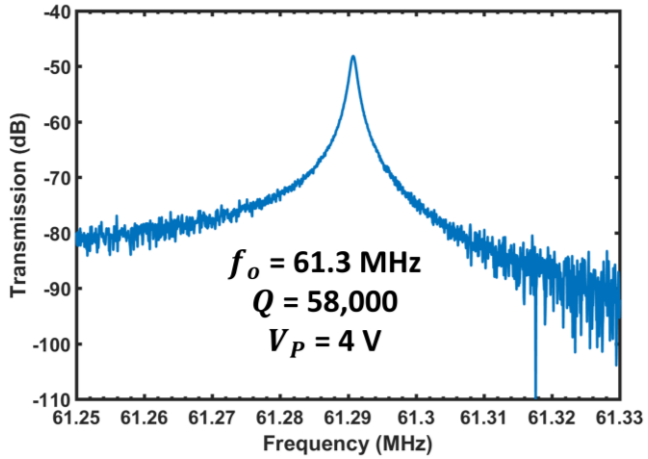

Fig. 7: Measured frequency response of the wine-glass disk resonator used in this work.

at the same frequency through all electrodes. The output current, upon conversion and amplification to a voltage signal, then yields the frequency characteristic in Fig. 7, measured with a dc-bias V_P of 4 V under 400 µTorr vacuum in a Lakeshore FWPX Vacuum Probe Station and showing a Q of 58,000 at 61.3 MHz.

V. Experimental Setup

Demonstration of the super-regenerative front-end of this work essentially used the setup in Fig. 1. Here, a Stanford Research Systems SG384 signal generator operating at twice the resonator's resonance frequency generates the parametric pump input. Applying this signal to the resonator structure through a bias-tee, alongside the dc-bias voltage V_P, allows for the strongest modulation of electrical stiffness due to the use of all four electrodes. An Agilent E5071C network analyzer then generates an input signal at frequency ω_o that drives one of the input electrodes, effectively serving as the injected signal. A Mini-Circuits RF amplifier senses the output current and routes it to an Agilent Infiniium oscilloscope for analysis. Varying the output power of the network analyzer amounts to varying the injected power to a super-regenerative front-end. If working properly, control of this injected power should control the oscillation growth and time-to-threshold, as needed for a super-regenerative front-end.

Parameter	Value	Unit
Disk radius, R_{disk}	32	µm
Nominal resonance frequency, f_{nom}	61.2	MHz
Disk thickness, t	2	µm
Electrode-to-resonator gap, d_o	58	nm
Electrode overlap angle, ϕ_e	76	°
Quality factor, Q	58,000	-
Young's modulus of polysilicon, E	158	GPa
Density of polysilicon, ρ	2,300	kg/m^3
Poisson's ratio of polysilicon, ν	0.226	-
Resonator DC-bias voltage, V_P	4	V
Static electrode-to-resonator capacitance (per electrode), C_o	25.9	fF
Electromechanical coupling factor, η_e	1.31×10^{-6}	C/m
Electromechanical coupling scalar, κ_i	0.731	-
Resonator dynamic mechanical stiffness, k_m	7.87×10^{5}	N/m
Resonator dynamic mass, m_{re}	5.33×10^{-12}	kg
Resonator damping factor, b_{re}	3.53×10^{-8}	kg/s

Table 1: Parameters of the wine-glass resonator used in this work, including device dimensions, material properties, biasing, and mechanical circuit parameters.

VI. Measurement Results

Fig. 8 presents oscilloscope pump and oscillation start-up waveforms for various in-channel input powers under the conditions of Table 1. Here, the amplitude of the pump signal at 122.6 MHz was 1.04 V, which corresponds to 15 µW of pump power into the resonator. This exceeds the threshold for parametric oscillation predicted by [10], which for the conditions of Table 1 stipulates the need for 830 mV of pump voltage amplitude to instigate parametric oscillation. Without an injected input, or with an off-resonance input (as would be the case for an FSK '0'), the waveform reaches 90% of steady-state in 1.34 ms.

On the other hand, the start-up waveforms with injected input powers ranging from −67 dBm to −27 dBm at the resonance frequency of the disk reach the 90% threshold much faster, down to 68 µs for the case of −27 dBm of input power. Even with −67 dBm, the growth reaches the 90% threshold in 1.32 ms, 20 µs earlier than the no-input case, which is reasonably

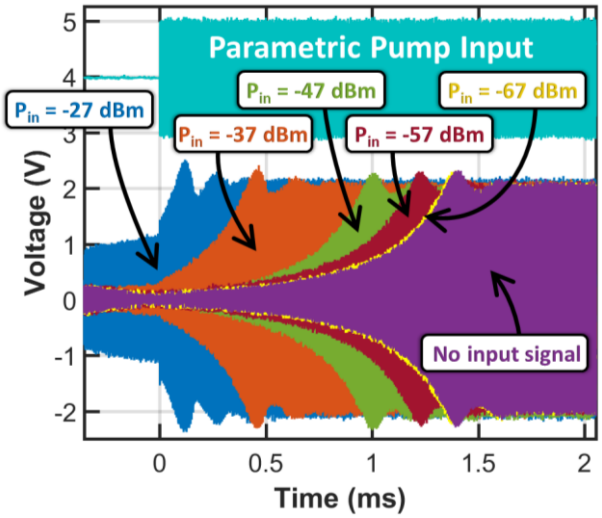

Fig. 8: Measured parametric pump and oscillation start-up transients seen at the device output for various in-channel signal powers applied to the input with a 1.04 V zero-to-peak pump signal applied to the disk structure. Since the frequency is high, the long time span hides sinusoidal waveform details, but their envelopes are clearly seen.

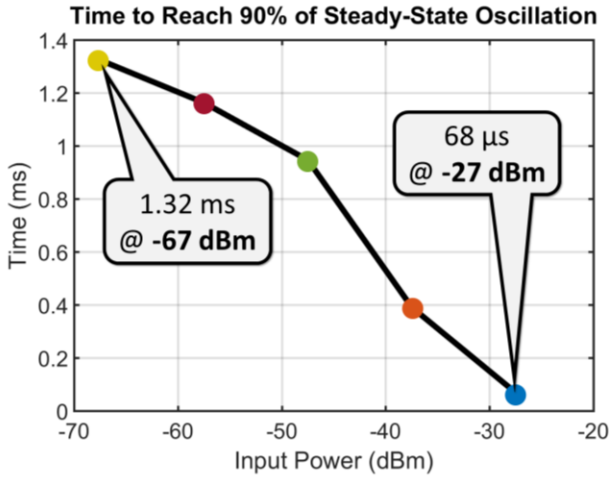

Fig. 9: Plot demonstrating the clear correlation between on-resonance input power and the amount of time it takes for the receiver to reach 90% of its steady-state. oscillation amplitude.

detectable even via the "eyeballing" of oscilloscope waveforms done here. More precise thresholding detection circuits, such as those used by [1], would of course be able to resolve even smaller time differences.

Fig. 9 finally plots time-to-the-90%-threshold versus resonance input power, clearly showing a marked dependence and revealing discernible time-to-threshold separations from the no-input case at least down to −67dBm. This means the receiver sensitivity must be at least −67dBm and will likely be found to be better upon more accurate bit-error-rate testing using thresholding circuits (rather than visual estimation from an oscilloscope waveform). Whatever the ultimate sensitivity, the presently demonstrated sensitivity is still very usable for IoT applications, which is impressive given use of a much simpler circuit realization with significantly lower power requirements.

VII. Conclusions

The ability of this parametrically pumped super-regenerative front-end to compete with a previous sustaining amplifier-based one [1] at considerably lower current draw gives it reasonable potential to supplant the previous implementation and perhaps become a preferred realization for MEMS-based super-regenerative receivers. The open-loop nature of this implementation also permits other benefits, e.g., more creative front-end filtering schemes to bolster the receiver against desensitization or increase its sustainable bit rate. Such additional flexibility over conventional super-regenerative receiver implementations might be key to achieving unique capabilities, especially if one desires greater channel switching and reconfigurability in multi-channel, multi-resonator MEMS-based transceiver realizations.

VIII. Acknowledgments

This material is based upon work supported by the National Science Foundation under Grant No. 1809319.

IX. References

[1] T. Rocheleau et al., "A MEMS-based tunable RF channel-selecting super-regenerative transceiver for wireless sensor nodes," in *Proceedings, Solid-State Sensors, Actuators, and Microsystems Workshop, Hilton Head*, Hilton Head Island, SC, June 8-12, 2014.

[2] Qualcomm, "CSR1010 datasheet," September 2012. [Online].

[3] L. Leene and T. G. Constandinou, "Time Domain Processing Techniques Using Ring Oscillator-Based Filter Structures," *IEEE Transactions on Circuits and Systems I: Regular Papers,* vol. 64, no. 12, pp. 3003-3012, Dec. 2017.

[4] G. G. Shahidi, "Chip Power Scaling in Recent CMOS Technology Nodes," *IEEE Access,* vol. 7, pp. 851-856, Dec. 10, 2018.

[5] F. W. Frink, "The basic principles of super-regenerative reception," *Proceedings of the Institute of Radio Engineers,* vol. 26, no. 1, pp. 76-106, January 1938.

[6] C. T.-C. Nguyen, "Micromechanical circuits for communication transceivers," in *Proceedings, 2000 Bipolar/BiCMOS Circuits and Technology Meeting (BCTM)*, Minneapolis, MN, Sept. 25-26, 2000, pp. 142-149.

[7] T. O. Rocheleau et al., "A micromechanical parametric oscillator for frequency division and phase noise reduction," in *2014 IEEE 27th International Conference on Micro Electro Mechanical Systems (MEMS)*, San Francisco, CA, pp. 210-213, Jan. 26-28, 2014.

[8] M. Faraday, "On a peculiar class of acoustical figures; and on certain forms assumed by a group of particles upon vibrating elastic surfaces.," *Philosophical Transactions of the Royal Society (London),* vol. 121, pp. 299-318, 1831.

[9] M. Akgul et al., "A negative-capacitance equivalent circuit model for parallel-plate capacitive-gap-transduced micromechanical resonators," *IEEE Transactions on Ultrasonics, Ferroelectrics, and Frequency Control,* vol. 61, no. 5, pp. 849-869, May 2014.

[10] T.-P. K. Nguyen, "Parametric oscillation with wine-glass disk resonators," Master's Report, University of California Berkeley, Dec. 2018.

[11] Y.-W. Lin et al.,"Series-resonant VHF micromechanical resonator reference oscillators," *IEEE Journal of Solid-State Circuits,* vol. 39, no. 12, pp. 2477-2491, Dec. 2004.

[12] J. Wang et al., "1.156-GHz self-aligned vibrating micromechanical disk resonator," *IEEE Transactions on Ultrasonics, Ferroelectrics, and Frequency Control,* vol. 51, no. 12, pp. 1607-1628, Dec. 2004.